

# Three-Dimensional Muscular Architecture of the Human Tongue Determined *In Vivo* With Diffusion Tensor Magnetic Resonance Imaging

Richard J. Gilbert, MD,<sup>1</sup> and Vitaly J. Napadow, PhD<sup>1,2</sup>

<sup>1</sup>Department of Mechanical Engineering, Massachusetts Institute of Technology, Cambridge, Massachusetts, and <sup>2</sup>Athinoula A. Martinos Imaging Center, Department of Radiology, Massachusetts General Hospital, Boston, Massachusetts, USA

**Abstract.** The myoarchitecture of the tongue is believed to consist of a complex network of interwoven fibers, which function together to produce a near limitless array of functional deformations. These deformations contribute mechanically to speech production and to oral cavity food handling during swallowing. We have previously imaged the 3D myoarchitecture of the mammalian tongue in excised tissue with diffusion tensor MRI, a technique which derives the 3D orientation of intramural fibers as a function of the extent to which a direction-specific MR signal attenuates under diffusion-encoding magnetic gradients. The resulting 3D diffusion tensor defines the relative orientations of the myofiber populations within a region of tissue. In this study, we have extended the use of this method to assess lingual myoarchitecture in normal human subjects *in vivo*. Subjects were imaged using a diffusion-sensitive stimulated-echo pulse sequence with single-shot echo-planar spatial encoding in the midsagittal plane. Differences in lingual fiber orientation were manifested by graduated changes in fiber direction throughout the tissue, without clear anatomical demarcations between regions of the tissue. The anterior tissue was composed generally of orthogonally oriented fibers surrounded by an axially oriented ring of tissue, whereas the posterior portion of the tissue was composed mostly of fibers projecting in the superior and posterior directions. The bulk of the tissue displayed a highly homogeneous, vertically oriented set of fibers, including the anteroinferior region of the tissue and extending nearly to the superior surface.

Further analysis of the tissue in terms of diffusion anisotropy demonstrated that the tissue could be represented by varying degrees of anisotropy, with a tendency toward high anisotropy in the dorsal and anteroventral periphery and low anisotropy in the central region of the tissue. These findings demonstrate that the muscular anatomy of the tongue can be displayed as a continuous array of structural units, or tensors, representing fibers of varying orientations throughout the tissue.

**Key words:** Lingual anatomy — Myoarchitecture — Magnetic resonance imaging — Deglutition — Deglutition disorders.

The human swallow is an instinctive and precisely orchestrated act with the goal of transporting food from the mouth to the esophagus [1,2]. During normal swallowing, the tongue first configures the ingested bolus in the oral cavity, and then propels the configured bolus from the oral cavity to the pharynx [3–5]. Clinically, abnormalities of tongue function are common and result in an inability to control an ingested bolus in the oral cavity, thus leading to impaired nutrition and uncontrolled exposure to an open or partially open airway [6,7].

The tongue is believed to consist anatomically of an interwoven three-dimensional (3D) network of skeletal muscle fibers and fiber bundles, involving both intrinsic fibers, i.e., those fibers possessing no direct connection to bony surfaces, and extrinsic fibers, i.e., those fibers possessing connections to bony surface [8–12]. It may be hypothesized that the intrinsic musculature consists of a core region of or-

thogonally aligned fibers, contained within a sheath-like tract of longitudinally oriented fibers. The intrinsic fibers are delicately merged with extrinsic muscles that modify shape and position from a superior direction (palatoglossus), posterior direction (styloglossus), and inferior direction (genioglossus and hyoglossus). Based on recent formulations [12], the merging of intrinsic and extrinsic fibers occurs along multiple geometric planes and appears to represent a union, rather than a simple overlay, of fibers. This fact places in question the classical anatomical distinction between “intrinsic” and “extrinsic” fibers, and it suggests that fiber orientation in the tongue may be considered more appropriately as graded variations of fiber orientation occurring throughout the body of the tissue.

A detailed study of lingual microstructure in humans may lead to a more robust modeling of lingual muscular physiology and dysfunction. Conventional imaging modalities, such as ultrasound and fluoroscopy, do not have the ability to infer intramural structure. In contrast, NMR imaging of the water diffusion tensor, a method termed diffusion tensor imaging, or DTI, has the capacity to noninvasively map fiber architecture *in situ* [13,14]. We have previously demonstrated that DTI can be used to resolve local fiber orientation for sheep and cow tongues *ex vivo* [15,16]. The current study extends this method by imaging the self-diffusion tensor field for lingual myoarchitecture *in vivo*, thereby opening up the possibility of interrogating 3D fiber architecture in normal humans and patients.

## Methods

Subjects ( $n = 3$ ) with no history of impaired speech or swallowing were chosen. The age range was 25–32 years, and the male–female ratio was 2:1. Normalization of tongue size relative to the length of the mandible was not performed because of the subjects’ high degree of size homogeneity and the relatively small sample size. These studies were approved by the Institutional Review Board for Human Research of the Massachusetts General Hospital.

### *Theoretical Basis of Diffusion Tensor Imaging*

Three-dimensional myoarchitecture of the tongue was derived by measuring spatially variant proton self-diffusivity with DTI. DTI derives diffusivity in tissues by the determination of NMR signal attenuation [13]. Diffusion is a physical property that represents the random translational motion of molecules. In the setting of biological tissues, NMR diffusion varies as a function of the position of cellular and subcellular barriers, as well as motion, temperature, and magnetic susceptibility. In the absence of macromolecular barriers, molecular diffusion would be equal in all directions (i.e.,

isotropy), whereas, when diffusion is hindered by the existence of cellular barriers, the pattern of molecular motion is unequal and tends to be greater along preferred directions (termed anisotropy) [17–19]. Since myocytes are characteristically elongated and cylindrically symmetric, cellular membranes impose significant barriers for the self-diffusion of free water in the transverse direction. The greater the hindrance to proton self-diffusion, the lower the magnetic resonance signal attenuation, a relationship that can be exploited to derive a spatially sensitive diffusion tensor. Signal attenuation receives contributions from both intracellular and extracellular fluid; however, the elongated geometry of muscle cells insures that both components induce maximal attenuation along the myofiber’s long axis [20]. In this manner, visualization of the self-diffusion tensor field can thus be utilized as an atlas of muscular tissue [15,16,21,22] as well as tissues from several other regions of the human body [17,18].

In order to obtain diffusivity data, transverse magnetization is systematically varied under the influence of a spatially dependent magnetic field by dephasing then rephasing the magnetic field. In the absence of motion, this action should result in complete phase coherence and no diffusion would be apparent. However, the presence of motion, presumably due to proton diffusion, would result in a loss of phase coherence and incomplete refocusing and thus yield an attenuation of the MRI signal. From the extent of signal attenuation, and taking into account  $T_2$  decay, an apparent diffusion coefficient can be calculated. The calculation of a diffusion coefficient in several directions (controlled by the spatially variant application of a magnetic field gradient) results in a unique array of 3D data for each voxel—the diffusion tensor. This symmetric second-order tensor can be conceived as a function of signal attenuation by

$$\ln\left(\frac{S_b}{S_0}\right) = -\sum_{i=1}^3 \sum_{j=1}^3 b_{ij} D_{ij}$$

where  $S_b$  is the signal-attenuated image,  $S_0$  is the unattenuated image,  $b_{ij}$  is the  $ij$  component of the classic  $\mathbf{b}$  matrix, and  $D_{ij}$  is the  $ij$  component of the diffusion tensor [14]. The  $\mathbf{b}$  matrix is a constant which is related to the direction-dependent diffusion sensitization and is expressed as

$$\mathbf{b} = \int \mathbf{k}^T \mathbf{k} dt$$

where the reciprocal space vector  $\mathbf{k}$  can be expressed as a function of the proton gyromagnetic ratio and the 3D diffusion sensitization gradient vector  $\mathbf{G}$ :

$$\mathbf{k} = \gamma \int \mathbf{G} dt$$

In order to efficiently span the 3D space of a given volume with diffusion sensitization gradients, seven images are acquired: six with gradient vectors toward the unopposed edge centers of a theoretical cube, and one unattenuated ( $\mathbf{G} = 0$ ) image. This results in a system of linear equations that can be solved for the diffusion tensor  $\mathbf{D}$  in the  $x, y, z$  coordinate system. This diffusion tensor is then transformed by solving  $\mathbf{D}\mathbf{v} = \lambda\mathbf{v}$  in order to place the diffusion tensor in the eigen coordinate system.

### *Technique for Diffusion-Weighted Magnetic Resonance Imaging*

Diffusion sensitization was achieved by proton spin preparation using stimulated echoes [20]. Stimulated echo sequences are preferable to their spin echo counterparts because they allow higher  $b$

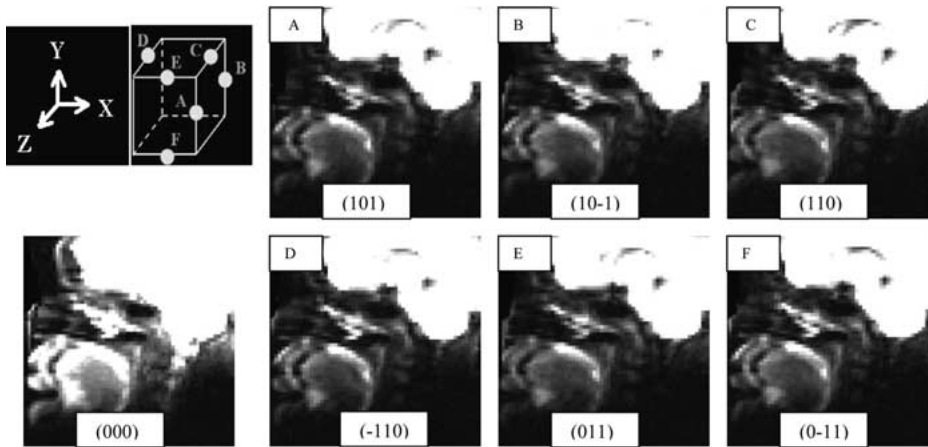


**Fig. 1.** Diffusion tensor imaging for quantification of 3D fiber organization. Diffusion-sensitized images are made by varying the magnetic field gradient  $G$ , one with  $G = 0$  and six with  $G$  oriented to the nonopposed edge centers of a cube. In each, the application of the diffusion gradient results in a unique signal attenuation that reflects the underlying orientation of the fibers within the voxel.

values to be realized with average magnetization gradients [20]. Furthermore, they allow for longer diffusion times because the longitudinal magnetization, which is used for the stimulated echo, is stored during the diffusion or mixing time and is not subject to transverse  $T_2$  decay. Stimulated echo sequences, however, have only half the signal-to-noise ratio (SNR) of spin echo techniques, necessitating signal averaging. Our stimulated echo sequence incorporated single-shot echo-planar spatial encoding with  $TE/TM/TR = 54/480/800$  ms, where  $TE$  is echo time,  $TM$  is mixing time, and  $TR$  is repetition time, and spatial resolution of  $3 \times 3 \times 6$  mm. Using 16 signal averages, acquisitions were completed in 3 min per slice yielding an SNR of approximately 40:1 (glossal-to-background magnitude ratio) in the unattenuated images  $S_0$  (diffusion-sensitizing gradients off) and a mean SNR of approximately 20:1 in the attenuated images  $S_b$  (diffusion-sensitizing gradients on) (Fig. 1).

A potential complication of diffusion-weighted imaging is the induction of image artifacts produced by eddy currents generated during the application of strong diffusion-sensitizing magnetic field gradients. Each on/off transition of the pulsed field gradient produced currents in the conductive portions of the magnetic bore, which oppose the change in magnetic field  $B$ . These currents generate a magnetic field, which can be modeled as a spatially variant decaying change in the static magnetic field  $B_0$

$$B(\mathbf{x}, t) = B_0 + \Delta B(\mathbf{x}) \sum_n s(n) \exp(-t/\nu)$$

Where  $\Delta B(\mathbf{x})$  is the eddy-current-induced magnetic field fluctuation and  $s(n)$  is the sign of the field, whether the gradient pulse was turned “on” or “off.” Thus,  $\Delta B(\mathbf{x})$  acts as an “unwelcome” imaging gradient that has the capacity to distort the  $k$ -space trajectory of the pulse sequence’s native imaging gradients. The specific distortion depends on the axis of the diffusion-encoding gradients inducing the eddy currents. In this regard, distortions of diffusion-weighted images produced by eddy currents may produce or modify the extent of diffusion anisotropy determined. In order to minimize the contribution of eddy currents, we adopted a pulse sequence which split the usual two long unipolar diffusion gradients into two bipolar gradients separated by another  $180^\circ$  refocusing pulse [21], thereby increasing the number of gradient transitions from  $n = 4$  to  $n = 8$ . This modification causes more transitions for a sequence of the same  $b$  factor. Furthermore, eddy currents from paired positive and negative transitions cancel more completely the more closely spaced they are temporally. Thus, by placing paired positive and negative gradient transitions closer together with this “double echo” pulse sequence, the induced eddy currents canceled each other out more completely, reducing artifactual image distortion.

The complete 3D diffusion tensor was computed for each image voxel and visualized as individual octahedra, whose axes were

scaled by the size of the eigenvalues and oriented along the corresponding eigenvectors (Fig. 2). Within the eigen coordinate system, the principal eigenvector,  $v_1$ , corresponded to the direction of greatest diffusion, or principal fiber direction, and was the major axis of the octahedron. The eigenvalues and eigenvectors for each diffusion tensor represented the magnitude and direction of maximal proton diffusivity, respectively. Octahedra were color-coded based on the principal eigenvector  $(x, y, z)$  triplet mapped to the red–green–blue color space:  $\{|v_{1x}|, |v_{1y}|, |v_{1z}|\} \in \{\text{red, green, blue}\}$ . Diffusion tensor anisotropy was quantified by the ratio of the greatest eigenvalue divided by the second largest eigenvalue of the diffusion tensor. This ratio constituted an anisotropy index, a measure that reflects the extent of orientational homogeneity for the fibers located within a specific region of tissue. In regions where most of the myofibers are oriented principally along the same axis, the anisotropy index will be high. Conversely, in tissue with many different myofiber orientations (e.g., multiple intertwined or overlaid fiber populations), the anisotropy index will be low. Because of the relatively small sample size used in this study, the attributes of the diffusion image, i.e., Principal fiber direction and diffusion anisotropy per voxel, were analyzed separately for each subject. Since aggregate data were not obtained, comparisons between individual subjects were qualitative.

The relatively low signal-to-noise ratio in the tongue required several methodological accommodations in order to achieve useful images, namely: (1) A compromise was achieved regarding optimal voxel size, which accounted for the need for longer total imaging times and larger voxel size to maximize signal-to-noise, on the one hand, with the need to reduce voxel size relative to the prior bovine images due to the smaller size of the human tongue,  $\sim 4 \text{ cm} \times 6 \text{ cm} \times 9 \text{ cm}$  for the human tongue compared with  $\sim 8 \text{ cm} \times 9 \text{ cm} \times 20 \text{ cm}$  for the bovine tongue. Thus, an upper limit for voxel size was used which maximized signal-to-noise while still providing adequate architectural discrimination. (2) Interimage voxel-to-voxel correspondence was achieved by requiring subjects to hold the tongue in a relatively steady position for 5 min while employing shallow respirations. Subjects were instructed to rest the tongue on the floor of the oral cavity during the entire scanning session. The use of head/neck surface coil facilitated increased stability of the mandible. Subjects were not precluded from clearing small volumes of saliva from the oral cavity as long as tongue motion was minimized.

## Results

Normal human subjects were studied with a diffusion-sensitive stimulated-echo pulse sequence, using a

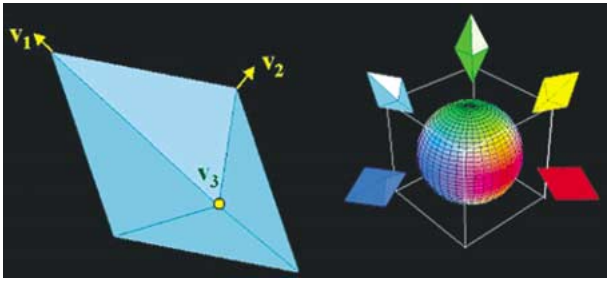


**Fig. 2.** Graphic visualization of the diffusion tensor. In order to display these data in 3D graphical form, the orientation-specific MR signals are aligned as tensors, with the  $x, y, z$  coordinates converted to eigen coordinates. The direction of greatest proton diffusion, the principal eigenvector of the diffusion tensor, corresponds to the predominant myofiber orientation within the voxel. The diffusion tensor is depicted as an octahedron, which is color-coded by the direction of the major axis (principal eigenvector).

single-shot echo-planar spatial encoding technique. Diffusion tensor imaging data was obtained from a midsagittal slice of the tongue (voxel size =  $3 \times 3 \times 8$  mm) *in vivo* and is shown graphically in Figure 3 as a series of spatially resolved octahedra representing the attributes of the individual tensors, i.e., principal fiber direction and the degree of fiber alignment (or diffusion anisotropy).

Our previous DTI study of the bovine tongue demonstrated that the tongue could be reasonably demarcated into regions, with the anterior tissue consisting of a central region of orthogonally oriented intrinsic fibers surrounded by an axially oriented muscular sheath, and the posterior tongue consisting predominantly of fibers originating at the inferior surface and projecting in a fan like manner in the superior, lateral, and posterior directions [16].

In the case of the human tongue, as shown in the current study, fiber direction was more aptly depicted by graded differences in fiber direction, without clear demarcations between muscles, an effect which was likely to be secondary to a relatively high degree of anatomical merging of fibers. The anterior portion of the tissue demonstrated a core region of orthogonally oriented fibers surrounded by an axially oriented muscular sheath, whereas the most posterior portion of the tissue manifested fibers originating at the inferior surface and projecting in superior and posterior directions. The bulk of the tissue manifested a highly homogeneous, vertically oriented set of fibers, which was likely to represent a merged combination of the extrinsic genioglossus fibers and the intrinsic verticalis fibers.

The fiber populations were further analyzed in terms of the homogeneity of their alignment by determining the extent of diffusion anisotropy at dis-

crete locations (Fig. 4). Anisotropy is a measure of the extent to which fibers are homogeneously aligned, with the highest anisotropy indicative of parallel alignment, usually present in the case of a single unidirectional fiber population, and the lowest anisotropy indicative of varying degrees of orthogonal fiber alignment, usually present in the case of multiple different fiber populations (with varying orientations in space) within a single sampled voxel. Depicting anisotropy in terms of gray-scale intensity, the tissue could be displayed as a continuously varying degree of anisotropy, with a tendency toward high anisotropy in the dorsal and antero ventral periphery and a tendency toward low anisotropy in the central (core) region of the tissue. Although explicit intersubject comparisons of diffusion attributes were not performed in this study, due to the small sample size, the above observations were consistent between subjects. Therefore, the findings of this study demonstrate the feasibility of defining lingual myoarchitecture in terms of graded variations in fiber direction and local alignment rather than in terms of discrete muscle boundaries.

## Discussion

The distribution and spatial orientation of muscle fibers in the tongue contribute substantially to its mechanical properties. The myoarchitecture of the tongue is believed to consist of a complex network of interwoven fibers and fiber bundles. By classical definitions, the lingual musculature comprises intrinsic fibers (fibers with no direct connection to bony surfaces) intricately merged with extrinsic fibers, which modify the shape and position of the tongue from the superior, posterior, and inferior directions. Lingual fibers may be arrayed within the tissue to generate a large variety of shape changes by virtue of the tissue's hydrostatic properties [23,24], thus accounting for its highly diverse physiological functions.

Because of the complex patterns of fiber alignment existing in the tongue, a method to assay the orientation of muscle fibers in the intact tissue should have benefit. We have previously examined intramural fiber organization of the mammalian tongue *ex vivo* through an imaging methodology that measures molecular diffusion as a function of direction-specific MR signal attenuation [15,16]. Because maximal diffusion occurs orthogonal to the short axis of most fiber-type cells, diffusion measurements can be used to derive quantitative information regarding three-dimensional fiber orientation. Thus, we exploited the measurement

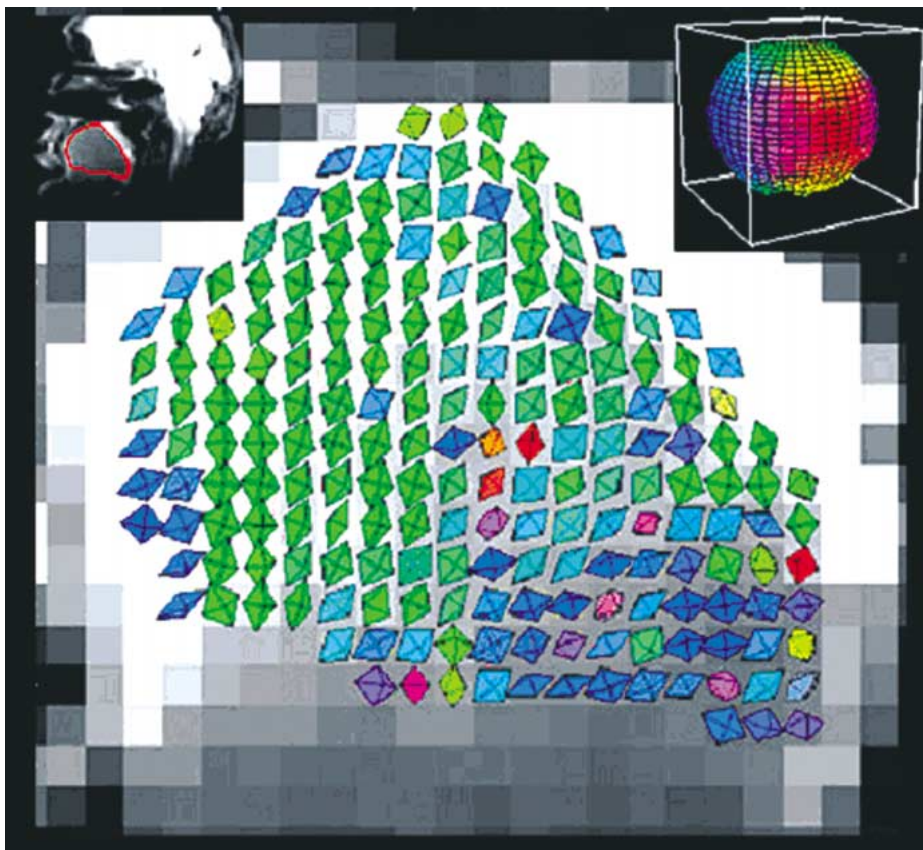


**Fig. 3.** *In vivo* DTI image of the human tongue. DTI was performed using a diffusion-sensitive stimulated-echo pulse sequence using single-shot echo-planar spatial encoding (see details of imaging in Methods). DTI data are depicted as the principal fiber direction for each voxel derived from a midsagittal slice of the tongue (voxel size =  $3 \times 3 \times 8$  mm) from the region shown in the upper left insert. Shown is a representative diffusion tensor image for a single subject. The image displays the DTI data as octahedra that have been color coded based on the principal fiber direction. This image displays a predominance of vertically and transversely oriented fibers in the core regions surrounded by a sheath of longitudinally oriented fibers on the superior and inferior surfaces.

of the self-diffusion tensor field to produce an anatomical display of lingual tissue in terms of the principal direction of its fibers and their degree of alignment. We have previously validated the methodology of DTI by qualitative correlation with lingual histology [15] and by deriving quantitative relationships between macroscopic and microscopic assays of 3D fiber orientation [25].

Our goal in the current report was to extend the technology of diffusion tensor imaging to the human tongue. We have shown here that diffusion tensor imaging is capable of representing 3D fiber organization in a single sagittal image plane *in vivo*. One key finding of this study is that the vertically oriented fibers, likely to comprise the genioglossus and intrinsic verticalis, are sufficiently merged (at the current resolution) so that a simplified characterization of discrete muscular populations is not feasible. This finding supports the notion that the tongue is best considered as a continuum of heterogeneously oriented muscular elements rather than a set of distinct muscles. Tissue deformation should result, therefore, from the activation of regionally defined fiber arrays of varying orientation, originating both within and outside of the body of the tongue.

A more subtle, yet important, method for distinguishing fiber orientation at the level of the voxel is diffusion anisotropy, a measure of the extent to which fibers within the voxel are similarly aligned. In other words, fiber regions displaying high anisotropy (such as the longitudinalis) are more likely to be aligned in a parallel manner, whereas fiber regions displaying low anisotropy (such as the overlapping fibers of the intrinsic core) are more likely to be aligned in an orthogonal manner. Quantitative relationships may exist between the extent of regional anisotropy and the force by which these regions contract. This possibility may have particular relevance when considering the behavior of tissue undergoing stimulated proliferation or pathological remodeling. Similarly oriented fiber bundles may either act *en masse* as contractile units or serve to localize a portion of a myofiber population's fibers into specific regions. In fact, during physiological motion, the efficient execution of different lingual tasks most likely uses a combination of both these strategies. For instance, in human swallowing, serially alternating transversus, verticalis, and genioglossus bundles may allow for the bolus-accommodating depression in the tissue to translate posteriorly, bringing food deeper into the oropharynx [26]. The high degree of struc-

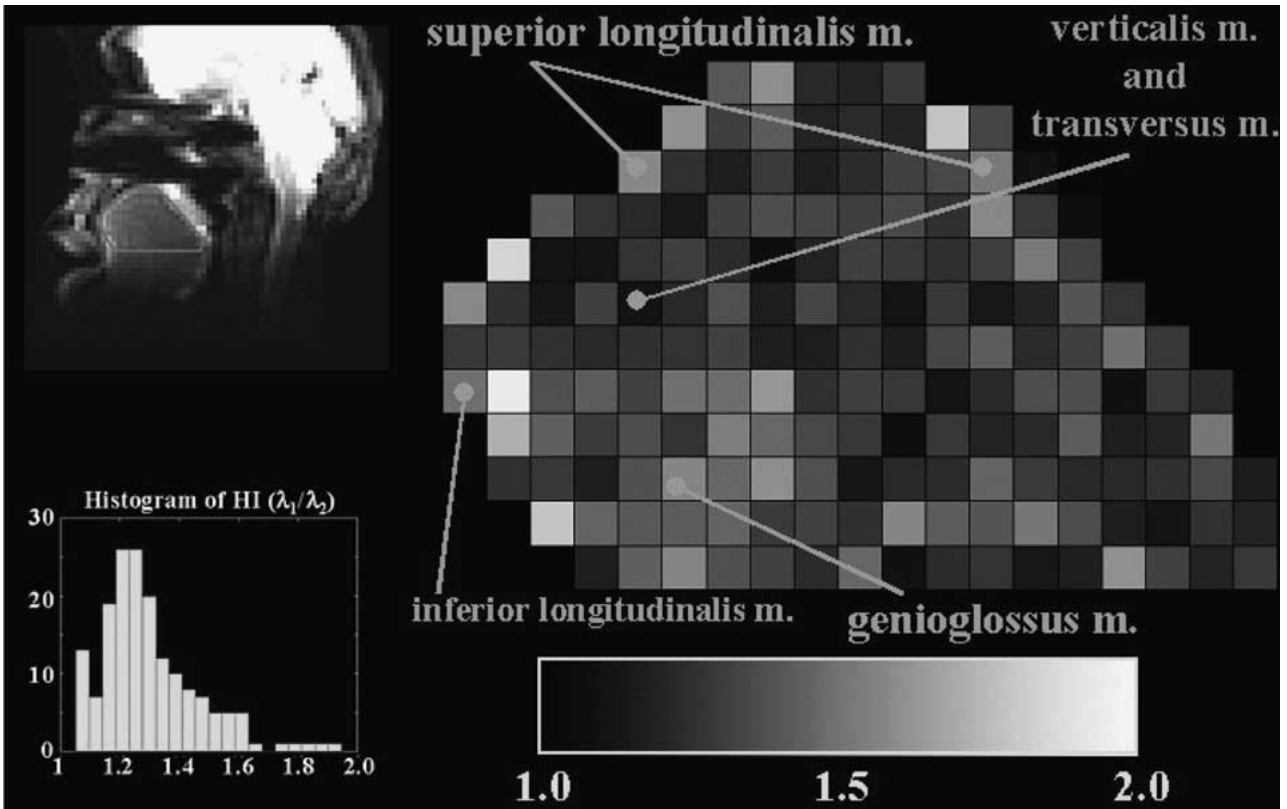


**Fig. 4.** Diffusion anisotropy map on tongue. Diffusion anisotropy ( $\lambda_1/\lambda_2$ ) was displayed as a gray-scale map with lighter voxels corresponding to higher anisotropy and darker voxels corresponding to lower anisotropy. Shown is a representative diffusion anisotropy map for a single subject. The analyzed region of interest was shown in the upper left. There was a region of high anisotropy (homogeneous fiber orientation) in the dorsal and anteroventral periphery and the anterior-inferior base. The central region possessed a generally lower anisotropy index (multiple myofiber populations). Although not determined experimentally, arrows indicate the approximate locations of conventional anatomic regions, such as the superior and inferior longitudinalis, the genioglossus, and the intrinsic core regions (transversus and verticalis), as a spatial point of reference.

tural redundancy existing in the tongue may have particular teleological importance given the vital role played by the tongue in humans for nutrition, respiration, and verbal communication.

In the application of DTI for lingual imaging, several methodologic limitations need to be considered. A principal limitation of the technique is the high degree of sensitivity of diffusion-weighted measurements to tissue motion. While the use of single-shot diffusion-weighted imaging compensates for most such motion, since it effectively “freezes out” the effects of motion, small degrees of motion are unavoidable and could have an effect on signal attenuation and the interpretation of the extent of diffusion anisotropy. In practice, most motion artifacts will provide a generalized effect on the diffusion signal and are not location-specific. Nonetheless, it may be necessary in the future to account for such artifacts by varying the size of the voxels sampled or modifying the pulse sequence in order to achieve valid diffusion tensors. A second limitation involves the inability to resolve *in vivo* the adequacy of directional resolution. We have previ-

ously related the extent of diffusion anisotropy exhibited by the diffusion tensor with the principal fiber direction shown in microscopically resolved 3D fiber alignment obtained via two-photon microscopy in resected lingual tissue [27]. These data indicated that the accuracy of the diffusion tensor in predicting fiber direction is greatest where diffusion anisotropy is high, i.e., most homogeneous alignment, and relatively reduced where diffusion anisotropy is low, i.e., least homogeneous fiber alignment. Because the current studies were performed *in vivo*, it is difficult to determine with certainty the accuracy of these tensors relative to their underlying myoarchitecture. Nevertheless, it is reasonable to consider that future variations of DTI will need to incorporate higher degrees of diffusive and angular resolution.

Although still preliminary, we believe that the measurement of local fiber direction through MRI may provide a way to characterize lingual muscular pathology. As an example, in patients with muscular dystrophy, lingual muscle fibers typically manifest reduced fiber diameter, increased cell necrosis, and the

large-scale replacement of contractile tissue with fat and connective tissue [28,29]. These effects may be associated with changes of local fiber organization, resulting in reduced diffusion anisotropy, i.e., increased randomness of fiber direction. Such disordered fiber alignment may, in turn, correlate with abnormalities in lingual shape and force production. In this way, the study of lingual fiber architecture may allow us to conceptualize lingual disease in terms of basic elements of structure and lead to a more robust understanding of lingual muscular dysfunction.

## References

1. Miller AJ: Deglutition. *Physiol Rev* 62(1):129–184, 1982
2. Groher M: *Dysphagia: Diagnosis and Management*, 3rd edn. Norwad, MA: Butterworth-Heinemann Press, 1997
3. Thexton AJ: Mastication and swallowing. *Br Dent J* 173:197–206, 1992
4. Palmer JB, Rudin NJ, Lara G, Crompton AW: Coordination of mastication and swallowing. *Dysphagia* 7:187–200, 1992
5. Gilbert RJ, Daftary S, Campbell TA, Weisskoff RM: Patterns of lingual tissue deformation associated with bolus containment and propulsion during deglutition as determined by echo-planar MRI. *J Magn Reson Imaging* 8:554–560, 1998
6. Maddock DM, Gilbert RJ: Quantitative relationship between liquid bolus flow and laryngeal closure during deglutition. *Am J Physiol* 265:G704–711, 1993
7. Paydarfar D, Gilbert RJ, Poppel CS, Nassab PF: Respiratory phase resetting and airflow changes induced by swallowing in humans. *J. Physiol (Lond)* 483:273–288, 1995
8. Abd-El-Malek S: Observations on the morphology of the human tongue. *J Anat* 73:201–210, 1939
9. Miyawaki K: A study of the musculature of the human tongue. *Annu Bull Res Inst Logopedics Phoniatrics Univ Tokyo* 8:23–50, 1974
10. Barnwell YM: Human lingual musculature: An historical review. *Int J Oral Myol* 2:31–34, 1976
11. Sonntag CF: The comparative anatomy of the tongues of mammalia. XII. Summary, classification, and physiology. *J. Zool Proc Zool Soc Lond* 21:701–762, 1923
12. Takemoto H: Morphological analyses of the human tongue musculature for three-dimensional modeling. *J Speech Lang Hear Res* 44:95–107, 2001
13. Stejskal EO: Use of spin echoes in a pulsed magnetic field gradient to study anisotropic, restricted diffusion and flow. *J Chem Phys* 43:3597–3603, 1965
14. Basser PJ, Mattiello J, LeBihan D: MR diffusion tensor spectroscopy and imaging. *Biophys J* 66:259–267, 1994
15. Gilbert RJ, Daftary S, Reese G, Weisskoff RM, Wedeen VJ: Determination of lingual myoarchitecture in whole tissue by NMR imaging of anisotropic water diffusion. *Am J Physiol* 175:G363–369, 1998
16. Wedeen VJ, Reese TG, Napadow VJ, Gilbert RJ: Demonstration of primary and secondary fiber architecture of the bovine tongue by diffusion tensor magnetic resonance imaging. *Biophys J* 80:1024–1028, 2001
17. Hajnal JV, Doran M, Hall AS, Collins AG, Oatridge A, Pennock JM, Young IR, Bydder GM: MR imaging of anisotropically restricted diffusion of water in the nervous system: technical, anatomic, and pathologic considerations. *J Comput Assist Tomogr* 15:1–18, 1991
18. Moseley MEJ, Kucharczyk J, Asgari HS, Norman D: Anisotropy in diffusion-weighted MRI. *Magn Reson Med* 19:321–326, 1991
19. Wu JC, Wong EC, Arrindell EL, Simons KB, Jesmanowicz A, Hyde JS: *In vivo* determination of the anisotropic diffusion of water and the T1 and T2 times in the rabbit lens by high-resolution magnetic resonance imaging. *Invest Ophthalmol Vis Sci* 34:2151–2158, 1993
20. Norris DG, Niendorf T: Interpretation of DW-NMR data: dependence on experimental conditions. *NMR Biomed* 8:280–288, 1995
21. Reese TG, Weisskoff RM, Smith RN, Rosen BR, Dinsmore RE, Wedeen VJ: Imaging myocardial fiber architecture *in vivo* with magnetic resonance. *Magn Reson Med* 34:786–791, 1995
22. Van Doorn A, Bovendeerd PH, Nicolay K, Drost MR, Janssen JD: Determination of muscle fibre orientation using diffusion-weighted MRI. *Eur J Morphol* 34:5–10, 1996
23. Smith KK, Kier WM: Trunks, tongues, and tentacles: moving with skeletons of muscle. *Am Sci* 77:29–35, 1989
24. Napadow VJ, Chen Q, Wedeen VJ, Gilbert RJ: Intramural mechanics of the human tongue in association with physiological deformations. *J Biomechan* 32:1–12, 1999
25. Napadow VJ, Chen Q, Mai V, So PTC, Gilbert RJ: Quantitative analysis of 3D resolved fiber architecture in heterogeneous skeletal muscle using NMR and optical imaging methods. *Biophys J* 80:2968–2975, 2001
26. Napadow VJ, Chen Q, Wedeen VJ, Gilbert RJ: Biomechanical basis for lingual tissue deformation during swallowing. *Am. J. Physiol* 40:G695–701, 1999
27. Napadow VJ, Chen Q, Mai V, So PTC, Gilbert RJ: Quantitative analysis of three-dimensionally resolved fiber architecture in heterogeneous skeletal muscle tissue using NMR and optical imaging methods. *Biophys J* 80:2968–2975, 2001
28. Yamanaka G, Goto K, Matsumura T, Funakoshi M, Komori T, Hayashi YK: Tongue atrophy in facioscapulohumeral muscular dystrophy. *Neurology* 28:733–735, 2001
29. Futo T, Kitaka T, Mizutani T, Okuyama H, Watanabe K, Totsuka T: Fatty acid composition of lipids in tongue and hindleg muscles of muscular dystrophic mice. *J Neurol Sci* 91:337–344, 1989